# Microsystems and Nanosystems

More information about this series at http://www.springer.com/series/11483

John A. Rogers · Roozbeh Ghaffari
Dae-Hyeong Kim
Editors

# Stretchable Bioelectronics for Medical Devices and Systems

Springer

*Editors*
John A. Rogers
University of Illinois at Urbana–Champaign
Urbana, IL
USA

Roozbeh Ghaffari
MC10 Inc.
Cambridge, MA
USA

Dae-Hyeong Kim
School of Chemical and Biological Engineering
Seoul National University
Seoul
Korea, Republic of (South Korea)

ISSN 2198-0063 ISSN 2198-0071 (electronic)
Microsystems and Nanosystems
ISBN 978-3-319-28692-1 ISBN 978-3-319-28694-5 (eBook)
DOI 10.1007/978-3-319-28694-5

Library of Congress Control Number: 2016932507



Printed on acid-free paper

This Springer imprint is published by Springer Nature
The registered company is Springer International Publishing AG Switzerland

# Contents

# Editors and Contributors

## About the Editors

**Prof. John A. Rogers** obtained B.A. and B.S. degrees in Chemistry and in Physics from the University of Texas, Austin, in 1989. From MIT, he received S.M. degrees in Physics and in Chemistry in 1992 and the Ph.D. degree in Physical Chemistry in 1995. From 1995 to 1997, Rogers was a Junior Fellow in the Harvard University Society of Fellows. He joined Bell Laboratories as a Member of Technical Staff in the Condensed Matter Physics Research Department in 1997, and served as Director of this department from the end of 2000–2002. He is currently Swanlund Chair Professor at University of Illinois at Urbana/Champaign, with a primary appointment in the Department of Materials Science and Engineering, and joint appointments in several other departments, including Bioengineering. He is Director of the Seitz Materials Research Laboratory. Rogers' research includes fundamental and applied aspects of materials for unusual electronic and photonic devices, with an emphasis on bio-integrated devices and bio-inspired designs. He has published more than 550 papers and is inventor on over 80 patents, more than 50 of which are licensed or in active use to various startups and large companies. Rogers is a Fellow of the IEEE, APS, MRS, and the AAAS, and he is a Member of the National Academy of Sciences, the National Academy of Engineering, the National Academy of Inventors, and the American Academy of Arts and Sciences. His research has been recognized with many awards, including a MacArthur Fellowship in 2009, the Lemelson-MIT Prize in 2011, the MRS Mid-Career Researcher Award and the Robert Henry Thurston Award (American Society of Mechanical Engineers) in 2013, the 2013 Smithsonian Award for Ingenuity in the Physical Sciences and the 2014 Eringen Medal of the Society for Engineering Science. He received an Honoris Causa Doctorate from the École Polytechnique Fédérale de Lausanne (EPFL) in 2013.

**Dr. Roozbeh Ghaffari** is Co-Founder and Chief Technology Officer at MC10 Inc. In this role, Roozbeh has shaped the technology vision of the company, and is responsible for defining and developing emerging products from concept phase through clinical validation. These efforts have led to the development and the launch of the BioStamp® and "tattoo-like" electronics as the foundation of MC10's wearable computing platforms. Prior to MC10 Inc., Roozbeh helped the launch of Diagnostics For All, a non-profit organization developing low-cost health diagnostics based on a patented microfluidics technology. Roozbeh is a Founding Editor of the MIT Entrepreneurship Review and is a research staff member at the MIT Research Laboratory of Electronics. Roozbeh's contributions in soft bioelectronics, micro/nano-scale systems, and auditory neuroscience research have been recognized with the MIT Helen Carr Peake Ph.D. Research Prize, the MIT100K Grand Prize, the Harvard Business School Social Enterprise Grand Prize, and the MIT Technology Review Magazine's Top 35 Innovators Under 35. Roozbeh has published over 40 academic papers and is inventor on over 40 patent applications and awards. Roozbeh holds B.S. and M.Eng. degrees in Electrical Engineering from the Massachusetts Institute of Technology, and a Ph.D. in Biomedical Engineering from the Harvard-MIT Division of Health Sciences and Technology.

**Prof. Dae-Hyeong Kim** obtained B.S. and M.S. degrees in Chemical Engineering from Seoul National University, Korea, in 2000 and 2002, respectively. He received Ph.D. degree in Materials Science and Engineering from University of Illinois at Urbana Champaign, in 2009. From 2009 to 2011, he was a postdoctoral research associate at University of Illinois. He is currently Associate Professor in the School of Chemical and Biological Engineering of Seoul National University. His research aims to develop technologies for high-performance flexible and stretchable electronic devices using high-quality single crystal inorganic materials and novel biocompatible materials that enable a new generation of implantable biomedical systems with novel capabilities and increased performance. In the area of clinical device research, a close collaboration with practicing cardiologists and neurologists demonstrated superb device performances for cardiac electrophysiology and brain–computer interfacing in vivo. These advanced diagnostic and therapeutic tools improve current surgical capabilities for treating cardiac, neural, and other fatal diseases. These achievements were published in high impact journals and honored through several awards. He has published more than 70 papers (including Science, Nature Materials, Nature Neuroscience, Nature Nanotechnology, Nature Communications, and PNAS), 30 international and domestic patents, and four book chapters. He has been recognized with several awards, including George Smith Award (2009) from the IEEE Electron Device Society, MRS Graduate Student Award (Gold Medal, 2009), Green Photonics Award from SPIE (2011), TR 35 award from MIT's Technology Review magazine (2011), and Hong Jin-ki Creative Award (2015).

## Contributors

**A.J. Aranyosi** MC10 Inc., Lexington, MA, USA

**Anthony Banks** Department of Materials Science and Engineering, Beckman Institute for Advanced Science and Technology, University of Illinois Urbana-Champaign, Urbana, IL, USA

**Jennifer Case** Purdue University, West Lafayette, IN, USA

**R. Chad Webb** 3M Company, Saint Paul, MN, USA

**Paolo DePetrillo** MC10 Inc., Lexington, MA, USA

**Michael D. Dickey** NC State University, Raleigh, USA

**Ray E. Dorsey** Department of Neurology, University of Rochester Medical Center, Rochester, NY, USA

**Roozbeh Ghaffari** MC10 Inc., Lexington, MA, USA

**Yonggang Huang** Department of Mechanical Engineering and Department of Civil and Environmental Engineering, Northwestern University, Evanston, IL, USA

**Yei Hwan Jung** Department of Electrical and Computer Engineering, University of Wisconsin-Madison, Madison, USA

**Hongki Kang** Department of Bio and Brain Engineering, Korea Advanced Institute of Science and Technology (KAIST), Daejeon, Republic of Korea

**Dae-Hyeong Kim** Center for Nanoparticle Research, Institute for Basic Science (IBS), Seoul, Republic of Korea; School of Chemical and Biological Engineering and Institute of Chemical Processes, Seoul National University, Seoul, Republic of Korea; Interdisciplinary Program for Bioengineering, Seoul National University, Seoul, Republic of Korea

**H.S. Kim** KU-KIST Graduate School of Converging Science and Technology, Korea University, Seoul, Republic of Korea

**I.Y. Kim** Department of Biomedical Engineering, Hanyang University, Seoul, Republic of Korea

**J.H. Kim** KU-KIST Graduate School of Converging Science and Technology, Korea University, Seoul, Republic of Korea

**Tae-il Kim** Department of Biomedical Engineering, Sungkyunkwan University (SKKU), Suwon, Korea; School of Chemical Engineering, Sungkyunkwan University (SKKU), Suwon, Korea; Center for Neuroscience Imaging Research (CNIR), Institute of Basic Science (IBS), Suwon, Korea

**Lauren Klinker** MC10 Inc., Lexington, MA, USA

**Ja Hoon Koo** Center for Nanoparticle Research, Institute for Basic Science (IBS), Seoul, Republic of Korea; Interdisciplinary Program for Bioengineering, Seoul National University, Seoul, Republic of Korea

**Rebecca Kramer** Purdue University, West Lafayette, IN, USA

**Siddharth Krishnan** Department of Materials Science and Engineering, University of Illinois at Urbana-Champaign, Urbana, IL, USA

**Stéphanie P. Lacour** School of Engineering, Centre for Neuroprosthetics, Bertarelli Chair in Neuroprosthetic Technology, Laboratory for Soft Bioelectronic Interfaces, Ecole Polytechnique Fédérale de Lausanne EPFL, Lausanne, Switzerland

**Chi Hwan Lee** Department of Materials Science and Engineering, Beckman Institute for Advanced Science and Technology, University of Illinois Urbana-Champaign, Urbana, IL, USA

**J.H. Lee** KU-KIST Graduate School of Converging Science and Technology, Korea University, Seoul, Republic of Korea

**Jongsu Lee** Center for Nanoparticle Research, Institute for Basic Science (IBS), Seoul, Republic of Korea; School of Chemical and Biological Engineering and Institute of Chemical Processes, Seoul National University, Seoul, Republic of Korea

**S.-H. Lee** KU-KIST Graduate School of Converging Science and Technology, Korea University, Seoul, Republic of Korea; Department of Biomedical Engineering, College of Health Science, Korea University, Seoul, Republic of Korea

**Darren J. Lipomi** Department of NanoEngineering, University of California, San Diego, CA, USA

**Clifford Liu** MC10 Inc., Lexington, MA, USA

**Nanshu Lu** Department of Aerospace Engineering and Engineering Mechanics, Center for Mechanics of Solids, Structures, and Materials, University of Texas at Austin, Austin, USA; Department of Biomedical Engineering, University of Texas at Austin, Austin, USA

**Yinji Ma** Department of Mechanical Engineering and Department of Civil and Environmental Engineering, Northwestern University, Evanston, IL, USA

**Zhenqiang Ma** Department of Electrical and Computer Engineering, University of Wisconsin-Madison, Madison, USA

**Moussa Mansour** Massachusetts General Hospital, Harvard Medical School, Boston, MA, USA

**Ryan McGinnis** MC10 Inc., Lexington, MA, USA

**Bryan McGrane** MC10 Inc., Lexington, MA, USA

**Ivan R. Minev** School of Engineering, Centre for Neuroprosthetics, Bertarelli Chair in Neuroprosthetic Technology, Laboratory for Soft Bioelectronic Interfaces, Ecole Polytechnique Fédérale de Lausanne EPFL, Lausanne, Switzerland

**Jeffrey B. Model** MC10 Inc., Lexington, MA, USA

**Mohammed Mohammed** Purdue University, West Lafayette, IN, USA

**Briana Morey** MC10 Inc., Lexington, MA, USA

**Brian Murphy** MC10 Inc., Lexington, MA, USA

**Yoonkey Nam** Department of Bio and Brain Engineering, Korea Advanced Institute of Science and Technology (KAIST), Daejeon, Republic of Korea

**Manuel Ochoa** School of Electrical and Computer Engineering, Purdue University, West Lafayette, IN, USA

**Timothy F. O'Connor** Department of NanoEngineering, University of California, San Diego, CA, USA

**Shyamal Patel** MC10 Inc., Lexington, MA, USA

**Rahim Rahimi** School of Electrical and Computer Engineering, Purdue University, West Lafayette, IN, USA

**Milan Raj** MC10 Inc., Lexington, MA, USA

**John A. Rogers** Department of Materials Science and Engineering, Beckman Institute for Advanced Science and Technology, University of Illinois Urbana-Champaign, Urbana, IL, USA

**Suchol Savagatrup** Department of NanoEngineering, University of California, San Diego, CA, USA

**Tsuyoshi Sekitani** The Institute of Scientific and Industrial Research, Osaka University, Osaka, Ibaraki, Japan

**Ellora Sen-Gupta** MC10 Inc., Lexington, MA, USA

**Nirav Sheth** MC10 Inc., Lexington, MA, USA

**Marvin Slepian** Sarver Heart Center, University of Arizona, Tucson, AZ, USA

**Donghee Son** Center for Nanoparticle Research, Institute for Basic Science (IBS), Seoul, Republic of Korea; School of Chemical and Biological Engineering and Institute of Chemical Processes, Seoul National University, Seoul, Republic of Korea

**Sung Hyuk Sunwoo** Department of Biomedical Engineering, Sungkyunkwan University (SKKU), Suwon, Korea; Center for Neuroscience Imaging Research (CNIR), Institute of Basic Science (IBS), Suwon, Korea

**Liu Wang** Department of Aerospace Engineering and Engineering Mechanics, Center for Mechanics of Solids, Structures, and Materials, University of Texas at Austin, Austin, USA

**John A. Wright** MC10 Inc., Lexington, MA, USA

**Shixuan Yang** Department of Aerospace Engineering and Engineering Mechanics, Center for Mechanics of Solids, Structures, and Materials, University of Texas at Austin, Austin, USA

**Michelle Yuen** Purdue University, West Lafayette, IN, USA

**Huilong Zhang** Department of Electrical and Computer Engineering, University of Wisconsin-Madison, Madison, USA

**Yihui Zhang** Department of Engineering Mechanics, Center for Mechanics and Materials, AML, Tsinghua University, Beijing, People's Republic of China

**Babak Ziaie** School of Electrical and Computer Engineering, Purdue University, West Lafayette, IN, USA

# Chapter 14
# In Vitro Neural Recording by Microelectrode Arrays

**Hongki Kang and Yoonkey Nam**

**Abstract** Neural interface plays an important role in monitoring and modulating brain activity. In order to study the neural information processing in vitro, microelectrode array (MEA) platform is used with cell culture or brain slice. To measure neural signals simultaneously from multiple cells for long-term period, extracellular neural recording technique is preferred and subcellular-scale microelectrodes, dense array, and flexible substrates are ideal. In this chapter, we will introduce the state-of-the-art in vitro neural recording technology based on microfabricated electrodes or transistors. MEAs with metal-type microelectrodes are passive types, and MEAs with active electronic components (field-effect transistors or integrated circuits) are active types. The motivation, operation principles, fabrication processes and materials, and current trends are reviewed.

**Keywords** Microelectrode array (MEA) · Neural interface · Neural recording · Action potentials · Extracellular recording

## 14.1 Introduction

Electrical signaling is one of the main components in the operation of nervous system. Neurons generate and conduct electrical signals. Because of the signal, we can think, remember, and move our bodies. The electrical signal generated by neurons is called action potential (AP). In our brain, there are over 100 billions of neurons forming over 100 trillions of synapses. In neural circuits, the APs generated at the membrane of neurons spread along the cell membrane, and they are transferred from one neuron to another at the synapse junctions using neurotransmitters. Therefore, technology is required to monitor and modulate the neural signals for

H. Kang · Y. Nam (✉)
Department of Bio and Brain Engineering, Korea Advanced Institute of Science and Technology (KAIST), Daejeon, Republic of Korea
e-mail: ynam@kaist.ac.kr



J.A. Rogers et al. (eds.), *Stretchable Bioelectronics for Medical Devices and Systems*, Microsystems and Nanosystems,
DOI 10.1007/978-3-319-28694-5_14

disease treatment, mind reading, and so on. In order to understand neural information processing mechanism, various types of neural tissue models are used: cell culture and brain slices. In case of cell culture models, a designated cell type is extracted from embryonic stage brain of rat or mouse and they are cultivated in an incubating condition to obtain an interconnected neural tissue. As for the brain slice, a brain is sliced into a thin piece that contains a circuit of interest, e.g., hippocampal circuits (e.g., DG–CA1, CA1–CA2) or thalamo-cortical circuits. To interrogate neural circuits, one need to measure action potentials from multiple sites or cells, which requires microelectrode arrays for the simultaneous access of neurons in the circuit. Moreover, microscale electrodes ('microelectrodes') are needed to record action potentials from a single cell. As the APs are only measured by directly measuring the membrane voltages, an alternative measurement technique that measures the extracellular field potential is often used. Extracellular recording technique gives an advantage of noninvasiveness to a single cell, and allows to acquire neural signals for long-term period, which makes it possible to investigate the change of neural firing during the development.

MEAs measure extracellular field potentials generated by action potentials and membrane currents and they are used for microstimulation by injecting charges through the same electrodes. MEAs can be classified into two types depending on the included functionality within the arrays: (1) active MEAs include active circuit elements such as amplifiers, analog-to-digital converter (ADC) or multiplexer (MUX) for signal amplification and data processing within the MEA chip itself; (2) passive MEAs are often composed of only passive electrodes on the MEA chip, which can detect and convey the neural signal to the external electronic system for further signal processing. In this chapter, we will review the electrical recording of neural signals using microelectrode arrays for in vitro neural tissues.

## 14.2 Passive Microelectrode Array Recording

Planar passive MEAs have become a promising experimental platform for electrophysiological studies of neural networks, ranging from dissociated cell cultures to slices of brain. MEA technology can provide very useful spatiotemporal measurement platform with simultaneous signal recording/stimulation from typically several tens of microelectrodes. The measurement can be noninvasive, allowing long-term recording and stimulation even for months. Planar passive MEAs interfaced with micron-scale cells using microfabricated multichannel metal electrode array on a rigid substrate such as glass or silicon wafer are shown in Fig. 14.1. Multielectrode channels are wired out and connected to external modules that are designed for neural signal amplification, filtering, data processing, and analysis.

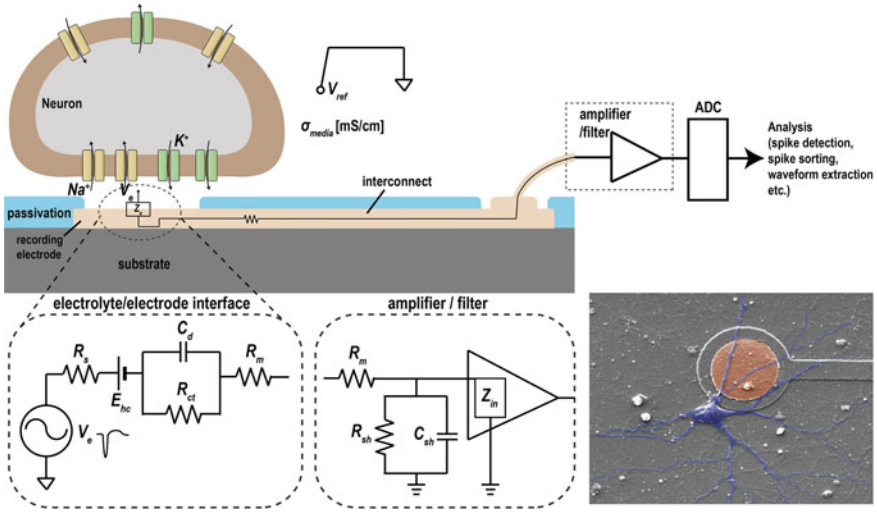


**Fig. 14.1** Schematic cross-section of passive MEA (not to scale). Electrical connection of overall system is described. An equivalent electrical circuit at the electrolyte/electrode interface is also described ($V_e$ extracellular potential (30–200 μV), $R_s$ solution resistance, $E_{hc}$ half-cell potential, $C_d$ double-layer capacitance, $R_{ct}$ charge-transfer resistance, $R_m$ metal interconnect resistance, $R_{sh}$ and $C_{sh}$ shunt resistance and capacitance for the amplifier, $Z_{in}$ input impedance of the amplifier, $V_{ref}$ reference voltage of the media bath)

### *14.2.1 Physics*

The electrolyte in extracellular fluid and metal recording electrodes form electrode–electrolyte interface where electrochemical reaction occurs. This interface can be simplified as an RC circuit with one resistor and one capacitor in parallel as shown in Fig. 14.1, which has different electrochemical interpretations. Electrons in the metal electrode can be transferred to the electrolyte by chemical oxidation or reduction of ions in the extracellular solution. This charge-transfer process (or faradaic process) by electrolysis is modeled as a charge-transfer resistor that determines the relationship between faradaic current and applied overpotential. On the other hand, even in the condition where charge-transfer cannot occur, capacitive currents can be generated due to the induced chemical species by the charges at the recording electrode. Depending on the types of the chemical species, characteristics of the adsorption are different. For instance, water molecules and ions form the first inner layer (called Helmholtz layer), which are adsorbed onto the interface. Other species such as solvated ions are attracted by long-range coulombic force forming diffusion layer. Since the amount of charges induced across the double layer vary by voltage, this non-faradaic capacitive current is characterized as double-layer capacitor ($C_d$). At the interface, electrochemical half-cell potential is formed and it depends on the type of metal electrode, surrounding ion concentration and temperature. As a result, extracellular field potential measurements using metal MEAs

suffer from the slow drift of poorly defined metal-electrolyte interface potential. In order to minimize electrochemical reaction at the interface, noble metal, such as platinum or gold, has been preferably used.

### 14.2.2 Fabrication and Materials

The most common microfabricated MEA structure is a patterned metal layer passivated by an insulating layer with only the measurement electrode areas exposed to the cells of interest. Conventional microfabrication processes are used to deposit and pattern the metal thin film. Since the cells need to stay alive on the passivation layer, the insulating layer (and also the exposed metal electrodes) must be biocompatible. Moreover, the insulating layer needs to have inert surface that does not react with abundant ions in the aqueous solution. Design parameters such as materials used for the electrode and passivation, the size of each electrode, inter-electrode spacing, and coverage area vary depending on the application and the type of cells of interest. After the microfabrication processes, the typical planar MEA is packaged onto a printed circuit board (PCB) such that the MEA can be connected to external circuits for further data processing. For in vitro experiments, a glass or teflon ring chamber that can keep cell culture medium is installed around the MEA.

As electrode materials, various metals such as platinum, gold, gold nanostructures, and aluminum, conductive polymers such as PEDOT (poly(3,4-ethylenedioxythiophene), transparent conductive oxides such as indium tin oxide (ITO), nanomaterials such carbon nanotube (CNT) or nanowire, and 2-D materials such as graphene, have been used. As insulator, silicon oxide, nitride, photoresists, parylene, PDMS, etc., have been used. As substrates, both rigid ones such as glass or wafer and flexible ones such as plastic, PDMS (polydimethylsiloxane) and parylene were used. See Table 14.1 for more details of recent developments.

### 14.2.3 Operation of Measurement Circuitry

The electrical recording of extracellular action potential signal measures the change of local electrical potential near a cell with respect to the reference electrode potential. In the measurement, the extracellular field potential can be modeled as a time-varying voltage source. In order to perform the voltage measurement, the fully fabricated and packaged passive MEA is typically connected with a multichannel amplifier unit that includes a bandpass filter with an appropriate range of passband frequency (e.g., 300 Hz–5 kHz for spikes, and 10–200 Hz for local field potentials) and a low noise amplifier (LNA) (e.g., gain: 1200 V/V). The processed signal after the amplifier unit is converted to digital signal by analog-to-digital converter

**Table 14.1** Recent development of passive and active MEAs

| Year | Ref. | Electrode material | No. of electrodes | Size[a] (μm) | \|Z\| @1 kHz (kΩ) | Electrode thickness (nm) | Insulator thickness (μm) | Substrate | In vitro testing[b] |
|---|---|---|---|---|---|---|---|---|---|
| 2009 | [14] | Au | 4096 | 21 (sq) | NA | Al | $SiO_2$ | CMOS | (r) Rat neurons (h) |
| 2009 | [47] | PtBK | 11,011 | 7 (dia) | NA | Pt (200) | $SiO_2$–$Si_3N_4$ (1.6) | CMOS | (r/s) Rat neurons (h) Brain slice |
| 2010 | [48] | Au spine | 62 | NA | NA | Au (45–65) | $SiO_2$ (0.3) | Glass | (r) Aplysia neuron |
| 2010 | [49] | Au nanoflake | 60 | 5–50 (dia) | 12–150 | Au (200) | $Si_3N_4$ | Glass | (r) Rat neurons (h) |
| 2010 | [50] | Au nanoporous | 64 (8 × 8) | 32 (dia) | 30 | Au (120) | SU-8 (2) | Glass | (r) Brain slice |
| 2011 | [7] | PEDOT :PSS | 60 | 120 (dia) | 400–1000 | PEDOT:PSS | PDMS | PDMS | (r) Brain slice |
| 2011 | [51] | Au nanopillar | NA | 15 (dia) | NA | Au (200) | ONO (0.8) | Si wafer | (r) HL-1 cell |
| 2012 | [5] | Si nanowire | 16 (4 × 4) | 0.15 (dia) 3 (H) | NA | Doped Si | $Al_2O_3$ (0.1) | Si wafer | (r) Rat neurons (h) |
| 2012 | [52] | Pt black | 64 | 30 (sq) | 100 | ITO | NA | Glass | (r) Mouse neurons (c) P19-derived neurons |
| 2012 | [53] | Pt nanopollar | 16 (4 × 4) | 0.15 (dia), 1.5 (H), 3 × 3 | 6000 | Pt (100) | $Si_3N_4$–$SiO_2$ (0.35) | Quartz | (r) Cardiac myocytes |
| 2013 | [54] | Au nanograin | 60 | 30 (dia) | 61 | Au (200) | $Si_3N_4$ (0.5) | Glass | (r/s) Rat neurons (h) |
| 2013 | [55] | CNT | 64 | 50 (sq) | NA | ITO | acrylic imide | Glass | (r) Rat neurons (h) |
| 2013 | [56] | PEDOT :PSS | 64 | 20 (sq) | 100 | ITO | – | – | (r) Rat neural stem cells |
| 2013 | [57] | PEDOT :PSS | 16 | 20 (sq) | 23 | Au (100) | Parylene (2) | Glass | (r) Rat brain slice |
| 2014 | [58] | IrOx nanotube | 64 | 34 $\mu m^2$ | NA | Pt (80) | $Si_3N_4$–$SiO_2$ (0.25/0.05) | Quartz | (r) Cardiac myocytes |

(continued)

**Table 14.1** (continued)

| Year | Ref. | Electrode material | No. of electrodes | Size[a] (μm) | \|Z\| @1 kHz (kΩ) | Electrode thickness (nm) | Insulator thickness (μm) | Substrate | In vitro testing[b] |
|---|---|---|---|---|---|---|---|---|---|
| 2014 | [59] | Pt nanocavity | NA | 12 (dia) | 200 | Pt | ONONO (0.8) | Glass | (r) HL-1 cell |
| 2014 | [60] | Doped diamond | 64 | 20 (dia) | NA | Doped diamond | SU-8 (1.5) | Si wafer | (r) HL-1 cell |
| 2014 | [11] | Pt | 26400 | 9.3 × 5.4 | NA | Pt | $SiO_2$–$Si_3N_4$ | CMOS | (r/s) Rabbit retina |
| 2015 | [9] | Au | 20 (4 × 5) | 30 (dia) | 7500 | Au | Parylene | Pary. (8 μm) | (r) Rat myocytes |
| 2015 | [61] | PEDOT-CNT | 59 | 30 (dia) | 19 | Au | – | Glass | (r/s) Rat retinal ganglion cells |
| 2015 | [8] | MWCNT | 16 | 100 (dia) | 55 | MWCNT | PDMS | Flex. | (r/s) Embryonic chick retina |
| 2015 | [62] | PtBK/pDA | 60 | 50 (dia) | 40 | Au (200) | $Si_3N_4$ (0.5) | Glass | (r/s) Rat neurons (h) |

*PET* Polyethylene terephthalate; *Pary.* Parylene; *Flex* various flexible substrates (adhesive tape, Pary., polyimide and PDMS)
*PtBK* platinum black; *pDA* polydopamine
[a]*dia* diameter; *sq* square
[b]*r* recording, *s* electrical stimulation, *h* primary hippocampal culture, *c* primary cortical culture

(ADC) and then analyzed further for spike detection, spike sorting, and waveform extraction. Although the amplitude of the extracellular potential is small (<1 mV), DC offset of the signal can be much higher and unpredictable due to the electrode–electrolyte interface half-cell potential and the cell/electrode junction potential. Therefore, capacitively coupled input terminal is preferred to filter the DC component of the input signal. For example, a cascaded current mirror operational transconductance amplifier where the input terminals are the gate terminal of metal–oxide–semiconductor field-effect transistors (MOSFETs), which is basically an open circuit, is used [1]. The high input impedance of the amplifier also helps to minimize any signal attenuation that occurs due to the voltage division by high impedance of the electrode–electrolyte interface. Therefore, in case of the voltage recording, this AC coupled LNAs leads to nearly zero DC current. Because the input node potential could be floating, measuring DC voltage signal such as resting potential would be very challenging. In case of electrical stimulation, it can be either high or low impedance node depending on the stimulation conditions (current-controlled or voltage-controlled) [2, 3].

### *14.2.4 High-Density Passive MEA*

While electrodes of cell size (i.e., tens of μm) are commonly used for recording, those electrodes cannot analyze local information of an individual neuron cell (e.g., propagation of AP along the dendrite, activity of ion channels in different locations on a cell and so on). Smaller electrodes, for instance in nano-scale, would allow the transition from large neural network to cellular level in-depth analysis. In addition, ideal goal would be to cover as large area as possible (potentially up to a size of primate brain) while maximizing the spatial resolution by high density and small electrodes.

In order to increase the electrode density, 256 or 512 channel microelectrodes were developed through standard photolithography. 256 channel MEAs are commercially available from multi channel systems (Reutlingen, Germany). The conductor line is ITO, and the electrode material is TiN. The spacing between the electrodes is as small as 30 μm, which is converted to the electrode density of 1,264 electrodes per $mm^2$ (=0.126 electrodes per 100 $\mu m^2$). 512 channel MEAs were reported by Mathieson et al. [4]. They used standard photolithography to pattern the ITO on a single plane. The electrode size was 5 μm and the inter-electrode spacing was 60 μm. The electrode density was 281 electrodes per $mm^2$ (=0.028 electrodes per 100 $\mu m^2$). There is a maximum density that can be obtained through a conventional single-layer metallization process. The line width and electrode size limit the minimal spacing.

Electrode size could be further reduced to nanometer scale through nanofabrication processes. Recently, nano-sized electrodes were developed using silicon nanowire (SiNW). Park's group integrated a group of silicon nanowires (9 wires in 16 $\mu m^2$) on a single electrode to improve the cell-electrode contact [5]. Cui's group

reported hollow-type iridium oxide nanotube electrodes to improve cell-electrode interface with high density (26 tubes per 100 $\mu m^2$) [6]. While these nanowire arrays showed significantly increased electrode density, each nanowire cannot independently operate as individual recording electrodes.

### *14.2.5 Flexible Passive MEA*

Flexible devices for neural recording are also of significant interest. When brain slices are used, especially, it is beneficial if the MEA is soft and flexible enough to have good pliability to form tight physical contact to the nonplanar surface of brain slice for better signal recording. Therefore, various flexible passive MEAs have been demonstrated: PEDOT electrodes on PDMS [7], CNT on various flexible substrates such as medical adhesive tape, Parylene-C, polyimide and PDMS [8], or gold thin film on Parylene-C [9]. Perforated flexible MEAs made of polyimide film was also developed to enhance the brain slice recoding through efficient oxygen supply [10].

## 14.3 Active Microelectrode Array Recordings

### *14.3.1 Motivation*

There are several expected advantages of the neural signal measurement by active MEAs compared to the passive ones. One of the motivations is to improve signal level by placing amplifiers such as transistors to cells as close as possible. The on-chip amplification and filtering right by the cells or at the recording sites could minimize noise signal generated from parasitics and interferences. Compact designs of the entire measurement platform within the chip area are also possible by the implementation of the circuit blocks on the integrated circuits (IC). These minimized measurement system area would be significantly beneficial, e.g., for implanted in vivo neural recording. Using state-of-the-art semiconductor technologies gives possibilities to add more functionalities on the same neural interface chip such as cyclic voltammetry, pH or temperature sensors, or light emitting diode (LED) array integration for optical stimulation. The active MEA could also enable unprecedentedly high electrode density through multiplexing of a number of electrodes for simpler data processing [11].

There are two types of active MEAs. The first type is to use field-effect transistors (FETs) at the cell-recording electrode interface as front-end amplifiers: neuron-FET coupling approaches have been explored since early 70s [12, 13]. The other is silicon complementary metal–oxide–semiconductor (CMOS) integrated circuits (IC)-based MEAs of which one of the main goals is to increase the spatial resolution of neural interface devices [14, 15].

### 14.3.2 Fabrication and Materials

When submicron CMOS technologies are used, fabrication of most active MEAs is done in commercial semiconductor foundries. However, since the final device structures and measurement environments are different from conventional CMOS processes (e.g., multiple recording electrodes opening in the center of the chip and their exposure to electrolyte, etc.), additional post-processing steps in research-oriented cleanroom facilities are often necessary. While those additional steps are not too much different from the passive MEA fabrication processes, more complexity and difficulty in the post-processing steps are expected due to the complex structure of the multilayer IC chips.

Silicon has been and will be the most widely used semiconductor materials in CMOS IC. In front-end-of-line (FEOL) of IC fabrication, highly-doped silicon or polysilicon are also used as conductive contacts or as resistors. Since gold creates deep-level traps in silicon, gold is not a CMOS compatible material for MOSFETs and in FEOL of IC process. As gate dielectric materials, high dielectric constant (high-k) insulator materials such as $HfO_2$ are used in more advanced technologies. In back-end-of-line (BEOL), copper and aluminum (or its alloy) are quite commonly used as interconnections. As described in Fig. 14.2, the top metal layer, which is usually composed of aluminum (or aluminum alloy) in conventional IC chips, is used for recording electrodes. Additional biocompatible metals such as gold, platinum, or platinum black can be either vacuum-deposited or electroplated onto the aluminum electrodes through post-processing [16–19]. Between metal stacks, low-k dielectric insulators are used to minimize parasitic interlayer capacitances. CMOS IC chips are typically passivated with silicon oxide and silicon nitride by plasma-enhanced chemical vapor deposition (PECVD) process, and lastly a polyimide layer. These insulation materials can be used to passivate the MEA but the exposed recording electrodes.

### 14.3.3 Physics

Fundamental physics governing the neuron-MEA interface in active MEAs varies depending on the types and the structures of the devices. Since CMOS MEAs have metal electrodes directly exposed to the cell, the same metal-electrolyte interface is formed as in passive MEAs, having double-layer capacitance and possible faradaic process [11]. On the other hand, most of FET-based MEAs reported so far have an insulation layer interfacing with the electrolyte instead (insulator-electrolyte interface). Therefore, electrolysis is prevented, and the capacitance of this insulation layer is dominant at the interface. There have been mainly two different structures of FET-based MEAs as shown in Fig. 14.2. One type is conventional MOSFETs without gate electrodes, thus neurons in direct contact with the gate dielectric [12, 13]. In this structure, gate dielectric capacitance coupling of the extracellular

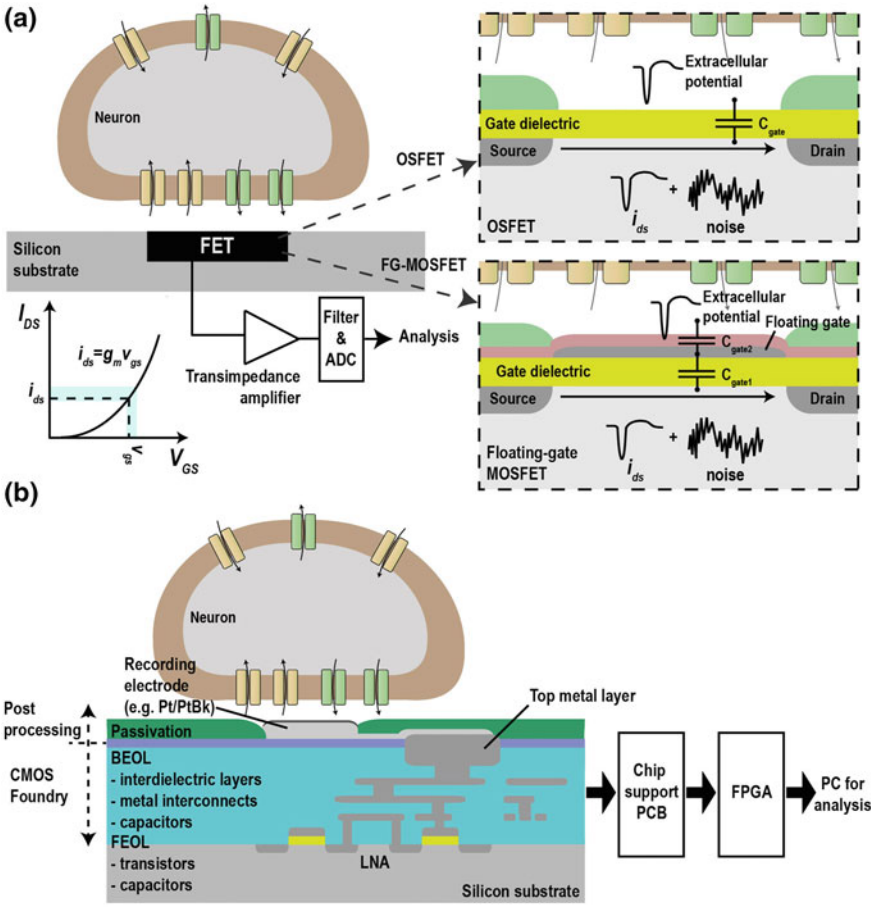


**Fig. 14.2** Schematic cross-section of active MEAs. (not to scale) **a** FET-based MEA. Recorded current signal by the FET is further amplified by transimpedance amplifier, and the amplified voltage signal is analyzed. Two common FET-based MEA structures are described: OSFET (MOSFET without gate metal) and FG-MOSFET (floating-gate MOSFET). *Inset graph on the left* describes the transfer characteristic of FETs that visualize how small voltage signal is converted to small drain current. **b** Schematic cross-section of high-density CMOS IC MEA. The top metal layer was used to define recording electrodes. The recorded signal is transferred to active low noise amplifier (LNA) circuits under the electrode area

potential with the transistor channel potential governs the signal recording. The other structure is the floating-gate MOSFETs [18, 20–22]. In this structure, either the actual gate or extended gate electrodes of MOSFETs are passivated with an insulation layer. Neurons are placed on top of the insulation layer. The neuron signal is, therefore, coupled to the transistor channel potential through two capacitors in series.

### 14.3.4 Operation of FET-Based MEA

The FETs used in active MEAs act as common-source amplifier which is a transconductance amplifier that converts the AC neural voltage signal at the gate terminal with respect to grounded source electrode to an amplified drain current signal that flows between drain and source electrodes as shown in Fig. 14.2a with the following relationship:

$$i_{ds} = g_m v_{gs} + i_{noise}$$

where $i_{ds}$ is drain current, $v_{gs}$ is neuron action potential at the gate, $g_m$ is transconductance defined as $\partial I_{DS}/\partial V_{GS}$, and $i_{noise}$ is mostly a combination of $1/f$ noise and thermal noise. In order to maximize the recorded signal, therefore, it is important to maximize the gain of the transistor ($g_m$), which is a function of various device parameters such as field-effect mobility, gate dielectric capacitance, geometry of the FET, DC biases, etc. While the transconductance is maximized at relatively high DC gate bias, non-zero DC bias at the gate is particularly not desirable in electrode–electrolyte interface due to the electrochemical corrosion. In depletion-mode MOSFETs that are already 'turned on' at zero gate bias, however, reasonably high transconductance can be achieved at zero gate bias. Cohen et al. suggested this approach to maximize the sensitivity of the neuron-FET interface and maximize the durability of the system [21].

Because of the weak neuron signal, minimization of intrinsic noise in MEAs is crucial. Unlike passive elements such as resistors that show thermal noise, in active electronic devices, $1/f$ noise (also called flicker noise) that shows $1/f$ behavior in its power spectral density is dominant in low frequency range where LFP and spikes are detected. Since the strength of $1/f$ noise is proportional to DC drain current due to more number of carrier electrons that can contributes to the noise, Cohen et al. also operated their FETs in lowest drain current condition to maximize signal-to-noise ratio (SNR) [21]. For silicon MOSFETs, it is known that the channel carriers are trapped/de-trapped by/from the traps within gate dielectric, causing fluctuation of drain current (thus, noise). Therefore, when OSFETs have the gate dielectric layer exposed to ions in electrolyte, the noise characteristics of the OSFETs could be degraded due to enhanced impurity scattering [23].

We can also think about the ideal electrical characteristics of the MEA at different levels. For FET-based active MEAs, in order to maximize SNR, the FETs must have maximum transconductance (e.g., from higher field-effect mobility) while minimizing lowest intrinsic noise signals. For example, transconductance value of 0.18 μm MOSFETs with typical width could be on the order of 100 μA/V which leads to tens of nA for extracellular voltage amplitude of ~100 μV. So, $1/f$ noise of those FETs in the frequency range from 10 Hz to 5 kHz must be smaller than a few nA. When new transistor technologies are adopted, these electrical characteristics must be carefully characterized. For the HD-MEAs, the on-chip front-end amplifiers must have the input-referred noise on the order of only a few μV or below to detect weak spikes as small as tens of μV.

### 14.3.5 SiNW-FET or Organic FET MEA

In order to reduce the recording area to nanoscale, nanoelectronic devices such as nanowire FETs (NWFETs) have been applied for neural recording devices [24–27]. With the usage of active nanoscale devices (as small as 10 nm) recording area can be reduced to several orders of magnitude from typical micron-scale MEAs. The small size of the device significantly increases the spatial resolution of MEAs and even allows the access of intracellular spaces for electrical recordings [27]. Nanowire devices could be fabricated on nonplanar flexible substrates. More details of the possibilities of nanoelectronic devices are summarized in [28].

As discussed in previous sections, FETs operate by the modulation of the channel conductance with respect to the change of gate field. It is shown that the change of extracellular field potential near the channel of NWFETs through gate capacitance coupling is converted to the change of channel conductance [29]. NWFETs reported in the work also have shown depletion-mode characteristics as was discussed in a previous section. Non-zero conductance of the channel and its slope allows the signal conversion at near zero gate bias. In other works, modified NWFETs are fabricated such that a small part of the channel area can be directly exposed to intracellular medium using vertical hollow probes [27].

Flexible organic FETs (OFETs) have also been suggested for neural signal recording and stimulation [30]. Unlike the previous FETs that use gate capacitance coupling for the extracellular signal to be converted to drain currents, in these OFETs, neurons are placed far away from the channel of the transistors on the opposite side of the gate electrode. However, relatively poor mobility of the organic semiconductor could be a concern because it could limit SNR and bandwidth of the recording system. On the other hand, unique characteristics of the novel materials could pave a new way of detection and add more functionality in neural interfaces. For example, the new interface between organic materials and biology has been studied and suggested for new applications [31–33]. Further, new fabrication methods such as various printing techniques that are compatible with flexible substrates and the new electronic materials can be used to open up new concepts of neural interface devices at lower fabrication costs.

### 14.3.6 High-Density CMOS MEA

The circuits designed for HD-MEAs are composed of buffer stage, amplifier, active (or passive) filters, multiplexer, and ADC. Different architectures of MEAs are well classified and summarized by Obien et al. [34]. The highest number of channel electrodes reported to date is 26,400 on $3.85 \times 2.1$ mm$^2$ sensing area from Ballini et al. [11]. With 17.5 μm electrode pitch, the electrode density is as high as near 3,200 electrodes per mm$^2$ (=0.32 electrode per 100 μm$^2$). Noise level of their system is 2.4 $\mu V_{rms}$ noise for AP band and 5.4 $\mu V_{rms}$ for LFP band. Choosing 10 bit

digital resolution and 20 kSamples/s, the IC chip recording 1024 electrodes (≈4 % of entire electrodes; 200 Mbit/s data rate) consumes 75 mW power. While the spatial resolution of electrodes is significantly improved, it is certain that adopting more advanced technology which is more energy efficient (e.g. 0.18 μm process that uses $V_{DD}$ of 1.8 V compared to 3.3 V used in this work [11]) is necessary to operate much more electrodes at the same time under tissue heating constraint [35]. More in-depth summary in MEA IC chips research can be found in this work [17].

Power consumption of the IC chip must be low to prevent thermal damage on neural tissues [36, 37]. Therefore, the range of aforementioned parameters will be fundamentally limited by the cell damage through heat dissipation and radiation. For example, if 25 kHz sampling rate is used with digital resolution of 10 bits, the data rate for a single channel is 250 kbit/s. For 1000 channels, the data rate increases to 250 Mbit/s. If on-chip data compression is implemented, we can reduce the data rate and thus power dissipation. However, the data compression circuit itself will also consume power. While the energy consumption per bit for efficient wired data transfer would be low, the power consumption constraint in, for example, fully implanted untethered in vivo measurement will be stricter. If 10 pJ/bit is consumed, overall power used for the 250 Mbit/s raw data transmission would be 2.5 mW. Harrison et al. reported a 100-electrode system designed for data rate of 330 kb/s and a 433 MHz transmitter consumed 13.5 mW of power [1]. As a point of reference, 12.4 mW power dissipated from a chip for 26 min showed 0.26–0.82 °C temperature increase in human bodies [38].

## 14.4 New Opportunities and Perspective

Various MEA technologies of both passive and active types are summarized in Table 14.1 for viewing the trend of recent development and comparison. As found in the table, different kinds and shapes of electrode materials have been adopted for better recording. Electrodes are getting smaller so that they can be packed much denser down to subcellular resolution. Nanoscale fabrication techniques are applied for higher sensitivity and spatial selectivity. In addition, not only rigid substrates but also flexible substrates are of interest for providing more in vivo-like environment to interface cells and tissues.

Flexible electronics have been of significant interests in both industries and academia. Flexible electronics is a very wide research field since virtually any technology that can offer mechanical flexibility can be called flexible electronics. In other words, it covers a wide range of applications. Even conventional micro/nanofabrication technologies such as CMOS can be a part of flexible electronics through extreme thinning of the semiconductor wafer because brittle inorganic semiconductor materials become flexible when they are thinned [39–41]. In addition to these conventional semiconductor fabrication processes, recent developments of new solution processable active electronic materials and new patterning methods of those materials have opened up much wider range of applications.

New materials such as nanoparticles, nanowires, organic semiconductor, conducting polymers, and graphene have been developed [42]. These new materials can also offer new functionalities such as chemical sensitivity which are useful for various sensor applications. New fabrication techniques such as inkjet printing have also offered biologically active material patterning for tissue engineering [43, 44]. With the growing interests in bioelectronics, wearable electronics and sensor applications of flexible electronics, there have been major developments in the application of flexible electronics technology to neural interface. To name a few, silk-based conformal microelectrode array, optical stimulator for optogenetic platform, flexible microelectrode array for bladder control, and so on [45, 46]. Flexible electronics technology could be the next key technology toward ultrasmall, ultradense, and ultrasoft in vitro neural interfaces in the future.

## References

1. R.R. Harrison, The Design of integrated circuits to observe brain activity. Proc. IEEE **96**, 1203–1216 (2008)
2. P. Fromherz, Electrical interfacing of nerve cells and semiconductor chips. Chem. Phys. Chem. **3**, 276 (2002)
3. P. Livi, F. Heer, U. Frey, D.J. Bakkum, A. Hierlemann, Compact voltage and current stimulation buffer for high-density microelectrode arrays. IEEE Trans. Biomed. Circ. Syst. **4**, 372–378 (2010)
4. K. Mathieson, S. Kachiguine, C. Adams, W. Cunningham, D. Gunning, V. O'Shea et al., Large-area microelectrode arrays for recording of neural signals. IEEE Trans. Nucl. Sci. **51**, 2027–2031 (2004)
5. J.T. Robinson, M. Jorgolli, A.K. Shalek, M.H. Yoon, R.S. Gertner, H. Park, Vertical nanowire electrode arrays as a scalable platform for intracellular interfacing to neuronal circuits. Nat. Nanotechnol. **7**, 180–184 (2012)
6. Z.L.C. Lin, C. Xie, Y. Osakada, Y. Cui, B.X. Cui, Iridium oxide nanotube electrodes for sensitive and prolonged intracellular measurement of action potentials. Nat. Commun. **5**, 3206 (2014)
7. A. Blau, A. Murr, S. Wolff, E. Sernagor, P. Medini, G. Iurilli et al., Flexible, all-polymer microelectrode arrays for the capture of cardiac and neuronal signals. Biomaterials **32**, 1778–1786 (2011)
8. M. David-Pur, L. Bareket-Keren, G. Beit-Yaakov, D. Raz-Prag, Y. Hanein, All-carbon-nanotube flexible multi-electrode array for neuronal recording and stimulation. Biomed. Microdevices. **16**, 43–53 (2014)
9. A. Mondal, B. Baker, I.R. Harvey, A.P. Moreno, PerFlexMEA: a thin microporous microelectrode array for in vitro cardiac electrophysiological studies on hetero-cellular bilayers with controlled gap junction communication. Lab Chip **15**, 2037–2048 (2015)
10. S.A. Boppart, B.C. Wheeler, C.S. Wallace, A flexible perforated microelectrode array for extended neural recordings. IEEE Trans. Biomed. Eng. **39**, 37–42 (1992)
11. M. Ballini, J. Muller, P. Livi, Y. Chen, U. Frey, A. Stettler, et al., A 1024-Channel CMOS microelectrode array with 26,400 electrodes for recording and stimulation of electrogenic cells in vitro. IEEE J. Solid-State Circ. **49**, 2705–2719 (2014)
12. P. Bergveld, J. Wiersma, H. Meertens, Extracellular potential recordings by means of a field effect transistor without gate metal, called OSFET. IEEE Trans. Biomed. Eng. **BME-23**, 136–144 (1976)

13. P. Fromherz, A. Offenhausser, T. Vetter, J. Weis, A neuron-silicon junction: a Retzius cell of the leech on an insulated-gate field-effect transistor. Science **252**, 1290–1293 (1991)
14. L. Berdondini, K. Imfeld, A. Maccione, M. Tedesco, S. Neukom, M. Koudelka-Hep et al., Active pixel sensor array for high spatio-temporal resolution electrophysiological recordings from single cell to large scale neuronal networks. Lab Chip **9**, 2644–2651 (2009)
15. U. Frey, U. Egert, F. Heer, S. Hafizovic, A. Hierlemann, Microelectronic system for high-resolution mapping of extracellular electric fields applied to brain slices. Biosens. Bioelectron. **24**, 2191–2198 (2009)
16. D.J. Bakkum, U. Frey, M. Radivojevic, T.L. Russell, J. Muller, M. Fiscella et al., Tracking axonal action potential propagation on a high-density microelectrode array across hundreds of sites. Nat. Commun. **4**, 2181 (2013)
17. A. Hierlemann, U. Frey, S. Hafizovic, F. Heer, Growing cells atop microelectronic chips: interfacing electrogenic cells in vitro with CMOS-Based microelectrode arrays. Proc. IEEE **99**, 252–284 (2011)
18. B. Eversmann, M. Jenkner, F. Hofmann, C. Paulus, R. Brederlow, B. Holzapfl et al., A 128 × 128 CMOS biosensor array for extracellular recording of neural activity. IEEE J. Solid-State Circ. **38**, 2306–2317 (2003)
19. I.L. Jones, T.L. Russell, K. Farrow, M. Fiscella, F. Franke, J. Müller, et al., A method for electrophysiological characterization of hamster retinal ganglion cells using a high-density CMOS microelectrode array. Front. Neurosci. **9**, (2015)
20. A. Offenhäusser, J. Rühe, W. Knoll, Neuronal cells cultured on modified microelectronic device surfaces. J. Vac. Sci. Technol., A **13**, 2606–2612 (1995)
21. A. Cohen, M.E. Spira, S. Yitshaik, G. Borghs, O. Shwartzglass, J. Shappir, Depletion type floating gate p-channel MOS transistor for recording action potentials generated by cultured neurons. Biosens. Bioelectron. **19**, 1703–1709 (2004)
22. S. Meyburg, M. Goryll, J. Moers, S. Ingebrandt, S. Böcker-Meffert, H. Lüth, et al., N-Channel field-effect transistors with floating gates for extracellular recordings. Biosens. Bioelectron. **21**, 1037–1044 (2006)
23. F.N. Hooge, 1/F noise sources. IEEE Trans. Electron. Devices **41**, 1926–1935 (1994)
24. B. Tian, T. Cohen-Karni, Q. Qing, X. Duan, P. Xie, C.M. Lieber, Three-Dimensional, flexible nanoscale field-effect transistors as localized bioprobes. Science **329**, 830–834 (2010)
25. F. Patolsky, B.P. Timko, G. Yu, Y. Fang, A.B. Greytak, G. Zheng, et al., Detection, stimulation, and inhibition of neuronal signals with high-density nanowire transistor arrays. Science **313**, 1100–1104 (2006)
26. Q. Qing, S.K. Pal, B. Tian, X. Duan, B.P. Timko, T. Cohen-Karni, et al., Nanowire transistor arrays for mapping neural circuits in acute brain slices. Proc. Nat. Acad. Sci. **107**, 1882–1887 (2010)
27. R. Gao, S. Strehle, B. Tian, T. Cohen-Karni, P. Xie, X. Duan, et al., Outside looking in: nanotube transistor intracellular sensors. Nano Lett. **12**, 3329–3333 (2012)
28. P.B. Kruskal, Z. Jiang, T. Gao, C.M. Lieber, Beyond the patch clamp: nanotechnologies for intracellular recording. Neuron **86**, 21–24 (2015)
29. M. De Vittorio, L. Martiradonna, J.A. Assad, *Nanotechnology and Neuroscience: Nano-Electronic, Photonic, and Mechanical Neuronal Interfacing* (Springer, New York, 2014)
30. V. Benfenati, S. Toffanin, S. Bonetti, G. Turatti, A. Pistone, M. Chiappalone, et al., A transparent organic transistor structure for bidirectional stimulation and recording of primary neurons. Nat. Mater. **12**, 672–680 (2013)
31. D. Ghezzi, M.R. Antognazza, R. Maccarone, S. Bellani, E. Lanzarini, N. Martino, et al., A polymer optoelectronic interface restores light sensitivity in blind rat retinas. Nat. Photon. **7**, 400–406 (2013)
32. G. Lanzani, Materials for bioelectronics: Organic electronics meets biology. Nat. Mater. **13**, 775–776 (2014)

33. V. Benfenati, N. Martino, M.R. Antognazza, A. Pistone, S. Toffanin, S. Ferroni et al., Photostimulation of whole-cell conductance in primary rat neocortical astrocytes mediated by organic semiconducting thin films. Adv. Healthc. Mater. **3**, 392–399 (2014)
34. M.E.J. Obien, K. Deligkaris, T. Bullmann, D.J. Bakkum, U. Frey, Revealing neuronal function through microelectrode array recordings. Syst. Biol. **8**, 423 (2015)
35. C.M. Lopez, A. Andrei, S. Mitra, M. Welkenhuysen, W. Eberle, C. Bartic et al., An implantable 455-Active-Electrode 52-Channel CMOS neural probe. IEEE J. Solid-State Circ. **49**, 248–261 (2014)
36. W.M. Reichert, *Indwelling Neural Implants: Strategies for Contending with the In Vivo Environment* (CRC Press, Boca Raton, 2008)
37. A. Denisov, E. Yeatman, Ultrasonic versus Inductive Power Delivery for miniature biomedical implants, in *2010 International Conference on Body Sensor Networks (BSN)*, 2010, pp. 84–89
38. K. Gosalia, J. Weiland, M. Humayun, G. Lazzi, Thermal elevation in the human eye and head due to the operation of a retinal prosthesis. IEEE Trans. Biomed. Eng. **51**, 1469–1477 (2004)
39. J.N. Burghartz, W. Appel, C. Harendt, H. Rempp, H. Richter, M. Zimmermann, Ultra-thin chip technology and applications, a new paradigm in silicon technology. Solid-State Electron. **54**, 818–829 (2010)
40. K. Kashyap, L.-C. Zheng, D.-Y. Lai, M. T. Hou, J.A. Yeh, Rollable Silicon IC wafers achieved by backside nanotexturing. IEEE Electron Device Lett. **36**, 829–831 (2015)
41. A.L.X. Jiang, L.C. Ming, J.C.Y. Gao, T.K. Hwee, silicon wafer backside thinning with mechanical and chemical method for better mechanical property (2006), pp. 1–4
42. W.S. Wong, A. Salleo, *Flexible Electronics: Materials and Applications* (Springer, New York, 2009)
43. P. Ihalainen, A. Määttänen, N. Sandler, Printing technologies for biomolecule and cell-based applications. Int. J. Pharm
44. U. Meyer, *Fundamentals of Tissue Engineering and Regenerative Medicine* (Springer, Berlin, 2009)
45. J.W. Lee, D. Kim, S. Yoo, H. Lee, G.-H. Lee, Y. Nam, Emerging neural stimulation technologies for bladder dysfunctions. Int. Neurourol. J. **19**, 3–11 (2015)
46. D.-H. Kim, J. Viventi, J.J. Amsden, J. Xiao, L. Vigeland, Y.-S. Kim, et al., Dissolvable films of silk fibroin for ultrathin conformal bio-integrated electronics. Nat. Mater. **9**, 511–517 (2010)
47. U. Frey, J. Sedivy, F. Heer, R. Pedron, M. Ballini, J. Mueller et al., Switch-matrix-based high-density microelectrode array in CMOS technology. IEEE J. Solid-State Circ. **45**, 467–482 (2010)
48. A. Hai, J. Shappir, M.E. Spira, In-cell recordings by extracellular microelectrodes. Nat. Methods **7**, 200–202 (2010)
49. J.H. Kim, G. Kang, Y. Nam, Y.K. Choi, Surface-modified microelectrode array with flake nanostructure for neural recording and stimulation. Nanotechnology, **21**, 85303, (2010)
50. E. Seker, Y. Berdichevsky, M.R. Begley, M.L. Reed, K.J. Staley, M.L. Yarmush, The fabrication of low-impedance nanoporous gold multiple-electrode arrays for neural electrophysiology studies. Nanotechnology **21**, 125504 (2010)
51. D. Bruggemann, B. Wolfrum, V. Maybeck, Y. Mourzina, M. Jansen, A. Offenhausser, Nanostructured gold microelectrodes for extracellular recording from electrogenic cells. Nanotechnology **22**, 265104 (2011)
52. Y. Takayama, H. Moriguchi, K. Kotani, T. Suzuki, K. Mabuchi, Y. Jimbo, Network-wide integration of stem cell-derived neurons and mouse cortical neurons using microfabricated co-culture devices. Biosystems **107**, 1–8 (2012)
53. C. Xie, Z. Lin, L. Hanson, Y. Cui, B. Cui, Intracellular recording of action potentials by nanopillar electroporation. Nat. Nanotechnol. **7**, 185–190 (2012)
54. R. Kim, N. Hong, Y. Nam, Gold nanograin microelectrodes for neuroelectronic interfaces. Biotechnol. J. **8**, 206–214 (2013)
55. I. Suzuki, M. Fukuda, K. Shirakawa, H. Jiko, M. Gotoh, Carbon nanotube multi-electrode array chips for noninvasive real-time measurement of dopamine, action potentials, and postsynaptic potentials. Biosens. Bioelectron. **49**, 270–275 (2013)

56. Y. Furukawa, A. Shimada, K. Kato, H. Iwata, K. Torimitsu, Monitoring neural stem cell differentiation using PEDOT–PSS based MEA. Biochimica et Biophysica Acta (BBA) - General Subjects, **1830**, 4329–4333 (2013)
57. M. Sessolo, D. Khodagholy, J. Rivnay, F. Maddalena, M. Gleyzes, E. Steidl et al., Easy-to-fabricate conducting polymer microelectrode arrays. Adv. Mater. **25**, 2135–2139 (2013)
58. Z.C. Lin, C. Xie, Y. Osakada, Y. Cui, B. Cui, Iridium oxide nanotube electrodes for sensitive and prolonged intracellular measurement of action potentials. Nat. Commun. **5**, 3206 (2014)
59. A. Czeschik, A. Offenhäusser, B. Wolfrum, Fabrication of MEA-based nanocavity sensor arrays for extracellular recording of action potentials. Physica Status Solidi (A) (2014)
60. V. Maybeck, R. Edgington, A. Bongrain, J.O. Welch, E. Scorsone, P. Bergonzo et al., Boron-doped nanocrystalline diamond microelectrode arrays monitor cardiac action potentials. Adv. Healthc Mater. **3**, 283–289 (2014)
61. R. Samba, T. Herrmann, G. Zeck, PEDOT–CNT coated electrodes stimulate retinal neurons at low voltage amplitudes and low charge densities. J. Neural Eng. **12**, 016014 (2015)
62. R. Kim, Y. Nam, Electrochemical layer-by-layer approach to fabricate mechanically stable platinum black microelectrodes using a mussel-inspired polydopamine adhesive. J. Neural Eng. **12**, 026010 (2015)